Prepared for submission to JCAP

Exploring the Dark Universe: Constraint on dynamical dark energy models from CMB, BAO and Growth Rate Measurements

Alexander Bonilla Rivera,[a,c,d,1] **Jorge García Farieta.**[a,b,d]

[a]Facultad Tecnológica, Unversidad Distrital Francisco José de Caldas, Carrera 7 No. 40B - 53, Bogotá, Colombia.

[b]Departamento de Física, Universidad Nacional de Colombia, Carrera 45 No. 26-85, Bogotá, Colombia.

[c]Grupo de Investigación en Física, Matemáticas y Computación (FizMaKo), Unversidad Distrital Francisco José de Caldas.

[d]Grupo de Investigación en Astronomía Sabio Caldas Universidad Distrital (AstroUD), Unversidad Distrital Francisco José de Caldas.

E-mail: abonillar@udistrital.edu.co, joegarciafa@unal.edu.co

arXiv:1605.01984v1 [astro-ph.CO] 6 May 2016

Abstract. In order to explain the current acceleration of the universe, the fine tuning problem of the value of Λ and the cosmic coincidence problem, different alternative models have been proposed. We use the most recent observational data from CMB (Plank 13 + WMAP 9) and LSS (SDSS, WiggleZ, BOSS, CMASS) to put cosmological constraints on different dynamical dark energy models. We employ the CMB Shift Parameter, which traditionally has been used to constrain the main cosmological parameters of the standard model ΛCDM. BAO data are also used including the cross-correlation WiggleZ-BOSS data (BW), which have the potential to strongly constrain the history of the cosmological expansion and the main properties of dark energy. Additionally we use data from Redshift-Space Distortions through Growth Parameter $A(z) = f(z)\sigma_8(z)$ to put constraints on the variance in mass fluctuations σ_8. We study the expansion history trougth H(z), q(z) and j(z) parameters (Obtained from an expansion in Taylor series of the scale factor $a(t)$) with data from BAO, where we found that at low redshift appears an peculiar behavior of slowdown of aceleration, which occurs only on dynamical dark energy models. On the other hand, using the Akaike and Bayesian Information Criterion (AIC, BIC) we found that ωCDM model is the most favored by the observational tests used in this work, including data from SNIa, GRBs, Strong Gravitational Lensisng (SGL) and gas mass fraction f_{gas} in galaxy clusters.

Keywords: Dark energy theory, Baryon acoustic oscillations, Cosmological parameters from LSS, cosmology of theories beyond the SM

[1]Alternative e-mail: alex.acidjazz@gmail.com

1 Introduction

At present day the concordance model ΛCDM is the most famous cosmological model, which together with the paradigm of inflation predicts the hierarchical structure formation, constituted of approximately 4% of luminous matter, 26% of dark matter (DM) and about 70% is a exotic component known as dark energy (DE) which it is traditionally presented as the main responsible for the late accelerated expansion of the Universe. In ΛCDM model, the DM is made up of colisionless non baryonic particles and the DE is provided by the cosmological constant Λ with an equation of state (EoS) $w = -1$. This model is in excellent agreement with the cosmological observations of the anisotropies of the cosmic microwave background (CMB) radiation, baryonic acoustic oscillations (BAO), Supernovaes Ia (SNIa), etc. Nevertheless, the standard model has some fundamental problems related to the nature of the dark matter and dark energy [5, 46]. In the context of DE, there are several theoretical arguments against a cosmological constant. One is the coincidence problem, that is, why today the value of dark energy density is of the same order of magnitude than dark matter density. Other important fundamental issue is the fine tuning of the present value of Λ which is completely in disagreement with the predictions of particle physics [38, 86]. Therefore, several dark energy models with a dynamical EoS have been proposed to alleviate the problems of the cosmological constant [46]. For instance, the EoS can be parametrizated in different ways, being one of the most popular the Chevallier-Polarski-Linder (CPL) [33, 58]. In addition, there are several models where a scalar field may play the role of the dark energy of the Universe, for example, the quintessence [27, 67], phantom [28, 34, 62], quintom [48] and k-essence fields [11, 12, 34]. On the other hand, a great number of theoretical models of dark energy consider interactions with dark matter (solve the problem of coincidence), e.g. Interacting Dark Energy [26], the Holographic dark energy (are free from the cosmological constant problem.)[35, 79–81, 90], modified gravity [42] and Braneworld models [47]. These models can be classified as phantom if EoS $\omega < -1$, or as quintessence if $\omega > -1$, where in the first case a fluid multicomponent is required with at least one phantom constituent, which has been shown to suffer from serious theoretical problems and the second case the general relativity needs to be extended to a more general theory on cosmological scales [60]. Among all these models we need to discriminate which one is the most favored by the current observations. The most popular method of discrimination is through the Akaike Information Criterion and Bayesian [3, 73, 75], which penalizes so much the number of data points as the number of parameters of each model. The most common tests comparing models with observations are SNIa, CMB, BAO,.., etc, which are considered as *geometric test* and determine H(z) independent of the validity of Einstein's equations, directly through the redshift dependence with cosmological distances (e.g. the angular diameter distance $d_A(z)$, the scale of the sound horizon $D_V(z)$ and mass gas fraction f_{gas}, among others). Other important observational methods to determine H(z) use *dynamics test*, which measure the evolution of the density of matter-energy (background or perturbations) and they are connected with geometry through a theory of gravity. An example of a dynamical test of geometry (H(z)) is the measured linear growth factor of the matter density perturbations D(a), whose measure can be obtained by different methods as redshift distortion factor in redshift surveys ($A(z) = f(z)\sigma_8(z)$), number counts of galaxy clusters ($dN(M,z)/dMdz$), large scale structure power spectrum (P(k)) and Integrated Sachs-Wolfe (ISW) effect. In this paper we include this dynamic test through data from $A_obs(z)$, which is important to know the effects of dark energy on the growth of structure (baryons and dark matter).

Our analysis begin with the cosmological models $\oint 2$, then we introduce the observational tests $\oint 3$, the statistical analysis of data $\oint 4$ and then we finish with the study of the history of expansion through the deceleration parameter $\oint 5$. In section $\oint 6$ we present the summary and discussion of results.

2 Cosmological models

In order to put constraints on DE cosmological models we need to calculate the theoretical angular diameter distance of the model and then compare it with the observations. The angular diameter distance for a Friedmann-Lemaitre-Robertson-Walker (FLRW) model universe, for a source at redshift z is

$$d_A(z,\Theta_i^m) = \frac{3000h^{-1}}{(1+z)}\frac{1}{\sqrt{\mid \Omega_k \mid}}\sin\varsigma\left(\int_0^z \frac{\sqrt{\mid \Omega_k \mid}}{E(z,\Omega_i)}dz\right), \tag{2.1}$$

where $h = H_0/100\text{kms}^{-1}\text{Mpc}^{-1}$ is dimensionless Hubble parameter and the function $\sin\varsigma(x)$ is defined such that it can be $\sinh(x)$ when $\Omega_k > 0$, $\sin(x)$ when $\Omega_k < 0$ and x when $\Omega_k = 0$ [52]. At present, all the signs of dark energy come from the measurements of expansion rate of the universe $H(z)$, which gives us its evolution and thus the history of the expansion. In standard FLRW cosmology, the expansion rate as a function of the scale factor $H(a)$ is given by the Friedmann equation as:

$$E^2(a,\Omega_i) = \Omega_r a^{-4} + \Omega_m a^{-3} + \Omega_k a^{-2} + \Omega_X e^{3\int_a^1 \frac{da'}{a'}(1+w(a'))} \tag{2.2}$$

where $H(a)/H_0 = E(a,\Omega_i)$, H_0 is the curent value of the expansion rate and the scale factor is related to redshift as $1+z = a^{-1}$. In the equation (2.2) Ω_i is the current energy density divided by today's critical density $\rho_{cri} = 3H_0^2/8\pi G$, In the form of the *i-th* component of the fluid density of: radiation (Ω_r), matter (Ω_m), curvature (Ω_k) and dark energy (Ω_X). The ratio of the pressure to the energy density $\omega(a) = p(a)/\rho(a)$ is the EoS of dark energy, the which divide our models into two cases: in one the energy density of the fluid is constant and in the other the energy density of the fluid is dynamic. In all cosmological models, the density parameter of curvature is free Ω_k and on which constraints are obtained. For each model of dark energy corresponds a vector of parameters $\Theta_i^{model} = \{\theta_i, \Omega_i\}$, where $\theta_i = \{h, \sigma_8\}$ and $\Omega_i = \{\Omega_r, \Omega_m, \Omega_k, \Omega_x\}$ is multicomponent fluid for the analysis of the present work.

2.1 ΛCDM model

We begin our analysis with the standard cosmological model. In this paradigm, the DE is provided by the cosmological constant Λ, with an EoS, such that $w = -1$. In this model the dimensionless Hubble parameter $E^2(z,\Theta)$ is given by

$$E^2(z,\Theta) = \Omega_r(1+z)^4 + \Omega_m(1+z)^3 + \Omega_k(1+z)^2 + \Omega_X, \tag{2.3}$$

where Ω_m and $\Omega_X = \Omega_\Lambda = 1 - \Omega_m - \Omega_k - \Omega_r$ are the density parameters for matter and dark energy respectively and Ω_r is the radiation parameter. The parameter vector is $\Theta_i^{\Lambda CDM} = \{h, \sigma_8, \Omega_m, \Omega_k\}$ and the best fit is shown in Table 1.

Λ *Cold Dark Matter model*	
h=0.6961 $\pm$ 0.0021	σ_8=0.761 $\pm$ 0.019
Ω_m=0.2867 $\pm$ 0.0032	Ω_k=0.00024 $\pm$ 0.0011

Table 1. Best fit parameters Θ_i with all data set to ΛCDM model.

Note that the parameter σ_8 enters into our analysis as a free parameter and from now in all cosmological models. This parameter represents the amplitude of the fluctuations of galaxies and is obtained from the Growth Parameter of structure $A_{obs}(z)$. Using a chi square estimate we find that $\sigma_8 = 0.761 \pm 0.019$ (see Figure 3, top-right), this result is compatible with the obtained from [1], [2], however PLANCK15 reports a lower uncertainty. Aditionally our best fit value for the dark energy density divided by the critical density today with 68% confidence is $\Omega_\Lambda = 0.7095 \pm 0.0054$, that is according with the limits reports by [2]. The value of cosmological constant in this work is positive and different from zero ($\Lambda = 1.5277 \pm 0.0092 \times 10^{-35} s^{-2}$), This value of Λ is consistent with measurements obtained by the High-Z Supernova Team and the Supernova Cosmology Project [65] [32]. Some derived parameters for this model are showed in Table 7.

To see the evolution of cosmic acceleration we plot the deceleration parameter q(z) in the Figure 4. As expected, q(z) has negative values at late times ($q_0 = -0.67$), and positive values at an earlier epochs. The transition from one decelerated expansion phase to an accelerated occurs at $z \sim 0.92$ using data from Baryon Acoustic Oscillations (BAO), in accordance with previous works [31].

2.2 wCDM model

An extension of the standard model where Λ has $w = -1$ is to consider that the EoS still is constant but its value can deviate of -1. In this case the dimensionless Hubble parameter $E^2(z, \Theta)$ for a FLRW universe with curvature reads as

$$E^2(z, \Theta) = \Omega_r(1+z)^4 + \Omega_m(1+z)^3 + \Omega_k(1+z)^2 + \Omega_X(1+z)^{3(1+w)}, \tag{2.4}$$

where $\Omega_X = (1 - \Omega_m - \Omega_k - \Omega_r)$. In this model the set of free parameters are $\Theta_i^{\omega CDM} = \{h, \sigma_8, \Omega_k, \Omega_m, \omega\}$. The best fit values are showed in the Table 2.

ω *Cold Dark Matter model*	
h=0.6945 $\pm$ 0.0021	σ_8=0.742 $\pm$ 0.020
Ω_m=0.2893 $\pm$ 0.0033	Ω_k=$-$0.0038 $\pm$ 0.0020
ω=$-$1.091 $\pm$ 0.031	

Table 2. Best fit parameters Θ_i with all data set to ωCDM model.

The Figure 3 shows the diagram of statistical confidence in the space of parameters (Ω_m - ω) (top-left) and (h - σ_8) (top-center) to ωCDM model, where we can see that ΛCDM model ($\omega = -1$) is discarded to 3σ combining all data sets. The result obtained in [75] ($w = -0.990 \pm 0.041$) is outside of our restriction to 3σ, however, the constraints obtained by [1] to ωCDM ($w = -1.13^{+0.13}_{-0.10}$) are in good agreement with our work to 1σ. Recently in

[2] the result obtained for the equation of state of the ωCDM model is $w = -1.006 \pm 0.045$, whose lower limit is consistent with our restriction to 2σ.

Figure 4 shows the evolution of the deceleration parameter q(z) as a function of redshift. A transition from one decelerated expansion phase to an accelerated occurs at $z \sim 0.86$ using only data from Baryon Acoustic Oscillations (BAO). Therefore ωCDM model predicts an accelerated expansion of the universe consistent with the cosmological observations, which is consistent with works previously reported [75].

2.3 Chevalier-Polarski-Linder model

Other extension to the standard scenario is allowing that equation of state of dark energy varyies with redshift via some parametrization. One of the most popular is the Chevallier-Polarski-Linder (CPL) parametrization [33] [58] given by

$$w(z) = w_0 + w_1 \frac{z}{1+z}, \tag{2.5}$$

where w_0 y w_1 are constants to be fitted. The dimensionless Hubble parameter $E(z)$ for CPL parametrization can be expressed as

$$E^2(z,\Theta) = \Omega_r(1+z)^4 + \Omega_k(1+z)^2 + \Omega_m(1+z)^3 + \Omega_X X(z), \tag{2.6}$$

where $\Omega_X = (1 - \Omega_k - \Omega_m - \Omega_r)$ and

$$X(z) = (1+z)^{3(1+w_0+w_1)} \exp\left[-\frac{3w_1 z}{1+z}\right]. \tag{2.7}$$

The free parameters to be constrained are $\Theta_i^{CPL} = \{h, \sigma_8, \Omega_k, \Omega_m, w_0, w_1\}$. The best fit values using all the observational tests are showed in the Table 3.

Chevalier-Polarski-Linder model	
h=0.6952 $\pm$ 0.0022	σ_8=0.737 $\pm$ 0.020
Ω_m=0.2897 $\pm$ 0.0038	Ω_k=$-$0.0080 $\pm$ 0.0024
ω_0=$-$0.90 $\pm$ 0.13	ω_a=$-$1.13 $\pm$ 0.85

Table 3. Best fit parameters Θ_i with all data set to *CPL* model.

The Figure 3 (down-left) shows the diagram of statistical confidence to 1, 2 and 3 sigma in the space of parameters $(\omega_a - \omega_0)$ for the CPL model. Note that the limits on h, Ω_m and σ_8 using all cosmological data are compatible with those obtained in [75] and [1]. However, there is tension for the constraints on Ω_k, ω_0 and ω_a, due to the degeneracy between the curvature and the state equation. Recently [1] combine Planck+WP+BAO gets $\omega_0 = -1.04^{+0.72}_{-0.69}$, which is in good agreement with our estimates. The CPL cosmological model is reduced to ΛCDM when $\omega_0 = -1$ and $\omega_a = 0$, however, we can see that the cosmological constant is outside the contour to 3σ in our analysis (Figure 3, down-left). The main physical parameters derived for this model are found in Table 7, which are very close to the reference model ΛCDM.

The point of transition from one decelerated phase to an accelerated phase occurs at $z \sim 0.85$ using only BAO data, which is showed in the Figure 4. Furthermore, there is a point at $z \sim 0.11$, where the expansion reaches its maximum acceleration, and then begin to slow down the acceleration at the current epoch ($q_0 = -0.48$). This slowing-down acceleration phase was found by [74] and [30] using SNIa data and recently by Cárdenas, Bernal & Bonilla [29] using only f_{gas}. This feature is presented as a anomalous behavior at low redshift [29] [59].

2.4 Interacting Dark Energy model

In interacting dark energy (EDE) models there is a relation between the energy density of dark energy ρ_x and the energy density of dark matter ρ_m that could alleviate the cosmic coincidence problem. For this, the general approach is common to introduce an interacting term in the right side of continuity equations in the following way [9, 25, 26, 39, 49]

$$\begin{aligned} \dot{\rho_m} + 3H\rho_m &= \delta H \rho_m, \\ \dot{\rho_x} + 3H\left(1+w_x\right)\rho_x &= -\delta H \rho_m, \end{aligned} \tag{2.8}$$

where w_x is the equation of state of dark energy and δ is a constant interacting term to be fitted with the observations. Thus, the dimensionless Hubble parameter for this interacting model is as follows

$$E^2(z,\Theta) = \Omega_r(1+z)^4 + \Omega_k(1+z)^2 + \Omega_m\Psi(z) + \Omega_X(1+z)^{3(1+w_x)}, \tag{2.9}$$

where $\Omega_X = (1 - \Omega_m - \Omega_k - \Omega_r)$ and

$$\Psi(z) = \frac{\left(\delta(1+z)^{3(1+w_x)} + 3w_x(1+z)^{3-\delta}\right)}{\delta + 3w_x} \tag{2.10}$$

This model is characterized by six parameters $\Theta_i^{IDE} = \{h, \sigma_8, \Omega_k, \Omega_m, w_x, \delta\}$. We show the best fit values of these parameters in Table 4.

Interacting Dark Energy model	
h=0.6873 $\pm$ 0.0028	σ_8=0.715 $\pm$ 0.019
Ω_m=0.3275 $\pm$ 0.0039	Ω_k=0.0030 $\pm$ 0.0022
ω_x=$-$1.059 $\pm$ 0.037	δ=$-$0.0063 $\pm$ 0.0024

Table 4. Best fit parameters Θ_i with all data set to *IDE* model.

In this case the Figure 3 (down-center) shows the parameter space for δ y ω_x at 1σ, 2σ and 3σ of statistical confidence. The ΛCDM is recovered when $\omega_x = -1$ and $\delta = 0$. however, our results show that the model ΛCDM is discarded to 3σ level of statistical confidence. On the other hand, If the term coupling in equation (2.8) takes on a negative value ($\delta < 0$) this corresponds to a transfer from dark matter to dark energy, whereas a positive coupling term ($\delta > 0$) implies the opposite and we can see that the transfer of dark matter to dark energy is favored in this work. The present analysis of the EoS of dark energy shows a phantom

behavior ($omega_x$ < -1), result consistent with those obtained by [75].

The transition state decelerated-accelerated occurs approximately at redshift $z \sim 1.06$ as can be observed in Figure 4, using only BAO data. The analysis of the deceleration parameter q(z) shows an anomalous behavior (slowdown of acceleration) at very low redshift (almost currently), which it is evident from the fast change of the slope of q (z) from $z \sim 0.5$ to $z \sim 0.0$.

2.5 Early Dark Energy model

In the early dark energy (EDE) scenarios it is proposed that the energy density of dark energy can be significant at high redshifts. This can be if the dark energy tracks the dynamics of the background fluid density [78, 87]. These models could ameliorate the coincedence problem of the cosmological constant. Here, we generalize the EDE model proposed by [40] adding a curvature term. The dimensionless Hubble parameter for this EDE model is

$$E^2(z,\Theta) = \frac{\Omega_r(1+z)^4 + \Omega_m(1+z)^3 + \Omega_k(1+z)^2}{1-\Omega_X}, \tag{2.11}$$

where Ω_X is given by

$$\Omega_X = \frac{\Omega_{X_0} - \Omega_e\left[1-(1+z)^{3w_0}\right]}{\Omega_{X_0} + f(z)} + \Omega_e\left[1-(1+z)^{3w_0}\right] \tag{2.12}$$

and

$$f(z) = \Omega_m(1+z)^{-3w_0} + \Omega_r(1+z)^{-3w_0+1} + \Omega_k(1+z)^{-3w_0-1} \tag{2.13}$$

such that $\Omega_{X_0} = 1-\Omega_m-\Omega_k-\Omega_r$ is the current dark energy density. Thus, we have five free parameters $\Theta_i^{EDE} = \{h, \sigma_8, \Omega_k, \Omega_m, \Omega_e, \omega_0\}$. The best fit of these parameters is shown in Table 5.

Early Dark Energy model	
h= 0.6850 ± 0.0029	σ_8=0.715 ± 0.019
Ω_m=0.3257 ± 0.0044	Ω_k=0.0040 ± 0.0024
ω_0=−1.101 ± 0.036	Ω_e=0.014 ± 0.010

Table 5. Best fit parameters Θ_i with all data set to *EDE* model.

Using the bayesian analysis we found $\Omega_e = 0.014 \pm 0.010$ (see Figure 3, down-right), which is in accordance with [40] reporting a $\Omega_e < 0.04$ by using a combination data from WMAP+VSA+CBI+ BOOMERANG+SDSS+SNIa and is also in agreement with [66], who reports a constraint $\Omega_e < 0.015$ at 95% confidence level. In Figure 3 (down-rigth) we can see that the model ΛCDM ($\Omega_e = 0$, $\omega_0 = -1$) is discarded even at 3σ.

The deceleration parameter $q(z)$ has a transition phase acelerated-decelerated to $z \sim 0.73$, moreover, q(z) shows the same anomalous behavior of slowdown of aceleration that CPL and IDE models for low redshift using only data from BAO, in this case at $z_{low} \sim 0.05$.

3 Cosmological test

Fluctuations in the matter and radiation density include dark matter Ω_m, baryon matter Ω_b and photons Ω_γ, which interact with each other through gravitational potential created by themselves [41, 56]. These fluctuations grow through gravitational instability as the universe expands, then decouple to form on the one hand, the Cosmic Microwave Background (CMB) and on the other hand, the Large Scale Structure (LSS) of the Universe. In the early universe the radiation was hot enough to ionize hydrogen and due to the Thomson scattering it is coupled to the baryons, forming one photon-baryon fluid. The radiation pressure of photons opposes the gravitational compression of the fluid producing a harmonic motion, whose amplitude perturbations does not grow but slowly decays, establishing thus the so-called Baryon Acoustic Oscillations (BAO). The gravitational driving force is due to the Newtonian potential, where overdensities of photon-baryon fluid produce oscillations, which determines the characteristic patterns of fluctuations in the power spectrum of matter and radiation [88]. Subsequently photons are diluted with the expansion and stream out of potential wells. Although effectively without pressure, the baryons still contribute to inertia and gravitational mass of fluid, which produces a change in the balance of pressure and gravity, then the baryons drag photons in potential wells. Previous to z_{drag}, perturbations in the photon-baryon fluid propagate as acoustic waves with speed of sound c_s, which at the epoch of drag define a sound comoving horizon r_s. At recombination epoch (z_{cmb}), photons decoupled from matter, where baryons can now constitute neutral elements and radiation is scattered for last time, forming the so-called CMB [41]. The resultant fluctuations in CMB, which are observed in radiation maps with anisotropy of the order of $\Delta T/T \sim 10^{-5}$, are better studied in its power spectrum.

In the following we present the details of the main observational sample: CMB by using Shift parameter R; BAO by means of Distance Ratio Scale $D_v(z)/r_s$ and growth of LSS through Redshift-Space Distortions $A(z) = f(z)\sigma_8(z)$, that we adopt in order to constrain the free parameters of the different cosmological models presented in the previous section, Including the calculation of some derived parameters which are presented in Table 6, with their corresponding definition and/or physical meaning.

3.1 CMB

A particular cosmological test to probe dark energy is the angular scale of sound horizon (r_s) at time of decoupling ($z_{cmb} \sim 1090$), the which is encrypted in the location l_1^{TT} of the first peak of the CMB power spectrum. We include CMB information of WMAP 9-yr and Planck 13 data [1, 51] to probe the expansion history up to the last scattering surface. The χ^2 for the CMB data is constructed as

$$\chi^2_{cmb} = X^T C^{-1}_{cmb} X, \tag{3.1}$$

where

$$X_{wmap9} = \begin{pmatrix} l_A - 302.40 \\ R - 1.7246 \\ z_{cmb} - 1090.88 \end{pmatrix}. \tag{3.2}$$

Here l_A is the "acoustic scale" defined as

Parameter	Physical meaning and/or definition
h	Dimensionless Hubble parameter
Ω_m	Dimensionless dark matter density parameter
Ω_Λ	Dimensionless dark energy density parameter to ΛCDM
Ω_k	Dimensionless curvature density parameter
σ_8	RMS matter fluctuations in linear theory
ω	Constant EoS to ωCDM
$\omega(a) = \omega_0 + (1+a)\omega_1$	EoS for *CPL* parametrization
ω_x, δ	EoS and dimensionless coupling term for *IDE*
ω_0, Ω_e	EoS and asymptotic dark energy density term for *EDE*
$H_0 = 100h$	Current expansion rate in $Km.s^{-1}Mpc^{-1}$
$t_0 = H_0^{-1}$	Age of the Universe today (in Gyr)
$\Omega_b = 0.045$	Dimensionless baryon density parameter
$\Omega_r = \Omega_\gamma(1 + 0.2271N_{eff})$	Dimensionless radiation density parameter
$\Omega_\gamma = 2.469 \times 10^{-5}h^{-2}$	Dimensionless photon density parameter
Ω_ν	Dimensionless neutrino density parameter ($\Omega_r = \Omega_\gamma + \Omega_\nu$)
$N_{eff} = 3.04$	Effective number of relativistic neutrino degrees of freedom
$\omega_m = \Omega_m h^2$	Physical dark matter density
$\omega_b = \Omega_b h^2$	Physical baryon density
$\rho_{cri} = 3H_0^2/8\pi G$	Critical density ($1.88 \times 10^{29} h^2 g/cm^3$)
Ω_X	Dimensionless dark energy density parameter
$\rho_X = \rho_{cri}\Omega_X$	Physical dark energy density
$\Lambda = 8\pi G\rho_\Lambda$	Cosmological constant where $\rho_\Lambda = \rho_{cri}3H_0^2$
c_s	Sound speed
r_s	Comoving size of sound horizon
z_{drag}	Redshift at which baryon-drag optical depth equals unity
$r_{drag} = r_s(z_{drag})$	Comoving size of the sound horizon at z_{drag}
$r_s/D_v(z)$	BAO distance ratio scale
z_{cmb}	Redshift at decoupled photon-baryon
$R(z_{cmb})$	Scaled distance at recombination (z_{cmb})
$l_A(z_{cmb})$	Angular scale of sound horizon at recombination (z_{cmb})

Table 6. Cosmological parameters used in the analysis. For each, we give the symbol and summary definition. The top block contains free parameters used for each cosmological model. The lower blocks define various derived parameters.

$$l_A = \frac{\pi d_L(z_{cmb})}{(1+z)r_s(z_{cmb})}, \tag{3.3}$$

where $d_L(z) = D_L(z)/H_0$ and the redshift of decoupling z_{cmb} is given by [54],

$$z_{cmb} = 1048[1 + 0.00124(\Omega_b h^2)^{-0.738}][1 + g_1(\Omega_m h^2)^{g_2}], \tag{3.4}$$

$$g_1 = \frac{0.0783(\Omega_b h^2)^{-0.238}}{1 + 39.5(\Omega_b h^2)^{0.763}}, g_2 = \frac{0.560}{1 + 21.1(\Omega_b h^2)^{1.81}}, \tag{3.5}$$

The "shift parameter" R defined as [22]

$$R = \frac{\sqrt{\Omega_m}}{c(1+z_{cmb})} D_L(z). \tag{3.6}$$

C^{-1}_{cmb} in Eq. (3.1) is the inverse covariance matrix, the wich is to WMAP9 data

$$C^{-1}_{cmb^{wmap9}} = \begin{pmatrix} 3.182 & 18.253 & -1.429 \\ 18.253 & 11887.879 & -193.808 \\ -1.429 & -193.808 & 4.556 \end{pmatrix}. \tag{3.7}$$

To Planck 13 data we obtained:

$$X_{Planck13} = \begin{pmatrix} l_A - 301.57 \\ R - 1.7407 \\ \omega_b - 0.02228 \end{pmatrix}, \tag{3.8}$$

where $\omega_b = \Omega_b h^2$ and $\Omega_b = 0.045$ for this work. The inverse covariance matrix for (l_A, R, ω_b) is how follow:

$$C^{-1}_{cmb^{Planck13}} = \sigma_i \sigma_j C_{NorCov_{i,j}}, \tag{3.9}$$

where $\sigma_i = (0.18, 0.0094, 0.00030)$ and normalized covariance matrix is

$$C_{NorCov_{i,j}} = \begin{pmatrix} 1.0000 & 0.5250 & -0.4235 \\ 0.5250 & 1.0000 & -0.6925 \\ -0.4235 & -0.6925 & 1.0000 \end{pmatrix}. \tag{3.10}$$

3.2 BAO

The large scale correlation function measured from 2dF Galaxy Redshift Survey and SDSS redshift survey, displays a peak which was identified with the expanding spherical wave of baryonic perturbations from acoustic oscillations at recombination and comoving scale of about $150h^{-1}Mpc$ [36, 44]. Baryon Acoustic Oscillations (BAO) are periodic fluctuations in the density of radiant matter (baryonic), which were printed in the primordial plasma (photon-baryon) before decoupling and as standard rules provide a powerful tool to measure the properties of dark energy [14, 88]. We use the recent results presented by Beutler et al. in [17]. The χ^2 for BOSS-WiggleZ (BW) BAO data is given by:

$$\chi^2_{BW} = (\bar{D}_{obs} - \bar{D}_{th}) C^{-1}_{BW} (\bar{D}_{obs} - \bar{D}_{th})^T, \tag{3.11}$$

where $\bar{D}_{obs} = (2056, 2132, 2100, 2516)Mpc = (CMASS - DR11, cc - BW, WiggleZ - BW, WiggleZ - hz)$ is data vector at $z = (0.57, 0.57, 0.57, 0.73)$ and $\bar{D}_{obs}$ is given by

$$\bar{D}_{obs} = D_v(z) \frac{r_s^{fid}}{r_s(z_d)} \tag{3.12}$$

where $r_s^{fid} = (149.28, 150.18, 150, 18, 148, 6)Mpc$ [17] and $r_s(z)$ is the comoving sound horizon

$$r_s(z) = c \int_z^\infty \frac{c_s(z')}{H(z')} dz', \tag{3.13}$$

where the sound speed

$$c_s(z) = \frac{1}{\sqrt{3(1+\bar{R}_b/(1+z)}}, \tag{3.14}$$

with $\bar{R}_b = 31500\Omega_b h^2 (T_{CMB}/2.7\text{K})^{-4}$ and $T_{CMB} = 2.726\text{K}$. The redshift z_{drag} at the baryon drag epoch is fitted with the formula proposed by [43],

$$z_{drag} = \frac{1291(\Omega_m h^2)^{0.251}}{1+0.659(\Omega_m h^2)^{0.828}}[1+b_1(\Omega_b h^2)^{b_2}], \tag{3.15}$$

where $b_1 = 0.313(\Omega_m h^2)^{-0.419}[1+0.607(\Omega_m h^2)^{0.674}]$ and $b_2 = 0.238(\Omega_m h^2)^{0.223}$. The matrix in equation (3.11) is

$$C_{BW}^{-1} = \begin{pmatrix} 250.47 & -3.48 & 0.09 & 0.004 \\ -3.48 & 36.32 & -5.67 & -4.79 \\ 0.09 & -5.67 & 4.27 & -3.26 \\ 0.004 & -4.79 & -3.26 & 18.90 \end{pmatrix} \times 10^{-5} \tag{3.16}$$

that it is the inverse of the covariance matrix

$$C_{BW}^{cov} = \begin{pmatrix} 400 & 56 & 88 & 29 \\ 56 & 4225 & 7410 & 2348 \\ 88 & 7410 & 40000 & 8772 \\ 29 & 2348 & 8772 & 7396 \end{pmatrix} \tag{3.17}$$

which is given by $C_{BW}^{cov} = \sigma_i \sigma_j R_{ij}$, where $\sigma_j = (20, 65, 200, 86)Mpc$ is the vector of variance and R_{ij} is the normalized correlation matrix given by:

$$R_{ij} = \begin{pmatrix} 1 & 0.043 & 0.022 & 0.017 \\ 0.043 & 1 & 0.57 & 0.42 \\ 0.022 & 0.57 & 1 & 0.51 \\ 0.017 & 0.42 & 0.51 & 1 \end{pmatrix} \tag{3.18}$$

which takes into account the BAO measurements from the cross-correlation between CMASS (BOSS) and the WiggleZ samples, including high redshift WiggleZ data point [17]. Similarly, for the SDSS DR7 BAO distance measurements, the χ^2 can be expressed as [64]

$$\chi^2_{SDSS} = (\bar{d}_{obs} - \bar{d}_{th}) C^{-1}_{SDSS} (\bar{d}_{obs} - \bar{d}_{th})^T, \tag{3.19}$$

where $\bar{d}_{obs} = (0.1905, 0.1097)$ is the datapoints at $z = 0.2$ and 0.35. $\bar{d}_{th}$ denotes the distance ratio

$$d_z = \frac{r_s(z_d)}{D_V(z)}. \tag{3.20}$$

Here, $r_s(z)$ is the comoving sound horizon as above. C^{-1}_{SDSS} in Eq. (12) is the inverse covariance matrix for the SDSS data set given by

$$C^{-1}_{SDSS} = \begin{pmatrix} 30124 & -17227 \\ -17227 & 86977 \end{pmatrix}. \tag{3.21}$$

For the 6dFGS BAO data [15], there is only one data point at $z = 0.106$, the χ^2 is easy to compute:

$$\chi^2_{6dFGS} = \left(\frac{d_z - 0.336}{0.015}\right)^2. \tag{3.22}$$

The total χ^2 for all the BAO data sets thus can be written as

$$\chi^2_{BAO} = \chi^2_{BW} + \chi^2_{SDSS} + \chi^2_{6dFGS}. \tag{3.23}$$

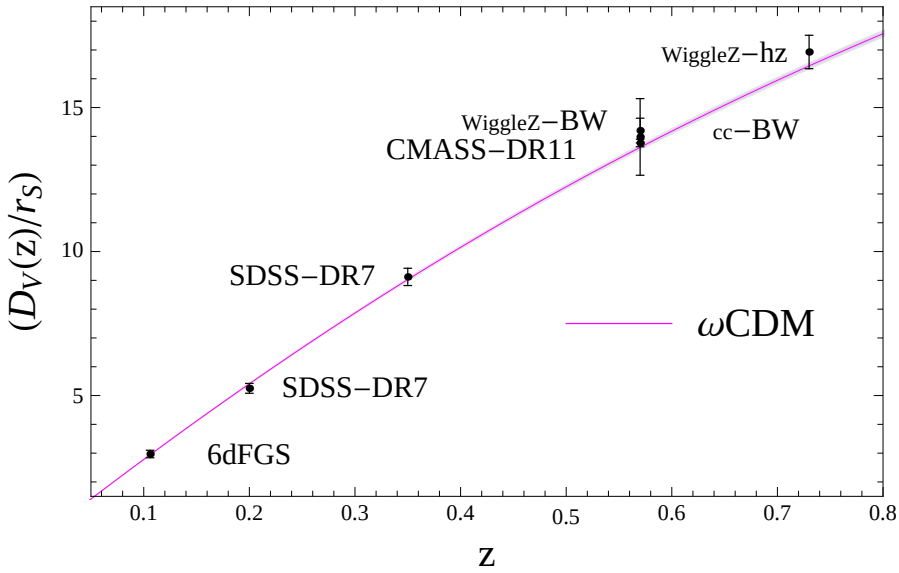

Figure 1. Plot of the distance-redshift relation from various BAO measurements $D_v(z)/r_s$. The gray area is the error propagation to $1-\sigma$ for the ωCDM model.

Figure 1 shows the Hubble diagram corresponding to the data points for BAO and the model that best fits to the data (ωCDM) with error propagation to $1-\sigma$.

3.3 LSS Growth Rate

The Large Scale Structure (LSS) of the universe is made up of huge empty, sheets, filaments, clusters of galaxies and superclusters, also known as cosmic web. These structures evolved from a homogeneous and isotropic universe and can in principle be treated theoretically as huge deviations from the mean density in the perturbation theory. We can define the linear matter density contrast as: $\delta(r,t) \equiv \delta\rho(r,t)/\rho(r,t)$, where $\rho(r,t)$ is the mean density of matter (background) and $\delta\rho(r,t)$ is the first order perturbation. The dynamics of the cosmic Hubble expansion H(t) is driven by the gravitational field of the mean matter density $\rho(r,t)$, while the density fluctuations $\delta\rho(r,t)$ produce an additional gravitational field. We can consider overdensed ($\delta\rho(r,t) > 0$) and underdensed regions ($\delta\rho(r,t) < 0$), e.g. super galaxy clusters and voids. In overdensed regions the gravitational field is stronger than in the cosmic average and therefore, due to this excess of self gravity, the overdensed region will expand more slowly than the average Hubble expansion. In an underdensed region the gravitational field is weaker than in the cosmic mean and therefore, the expansion is slow down less than in the cosmic mean. Overdense regions increase their density contrast over the course of time,

while underdense regions decrease their density contrast. In both situations, $|\delta|$ increased with time. Then, the characterization of growth of the density perturbations can be made assuming the following relationship $\delta(r,t) = D(t)\delta_0(r)$, where $D(t)$ is the linear Growth Factor Structure and $\delta_0(r)$ is an arbitrary function of the spatial coordinate. Under the assumption that general relativity is the correct theory of gravity ($G_{eff}(a) = 1$) [61, 77, 84], we use $D(a)$ in order to characterize the growth of structure, which is obtained numerically of the following differential equation:

$$\ddot{D}(a) + \left(\frac{3}{a} + \frac{\dot{H}(a)}{H(a)}\right)\dot{D}(a) - \frac{3}{2}\frac{\Omega_m}{a^5 H(a)^2} G_{eff}(a) D(a) = 0 \tag{3.24}$$

where dots denote differentiation with respect to the scale factor and we assume the initial conditions $D(0) = 0$ and $\dot{D}(0) = 1$ for the growing mode. the solution $\delta(r,t) = D(t)\delta_0(r)$ indicates that in linear perturbation theory the spatial shape of the density fluctuations is frozen in comoving coordinates and only their amplitude increases.

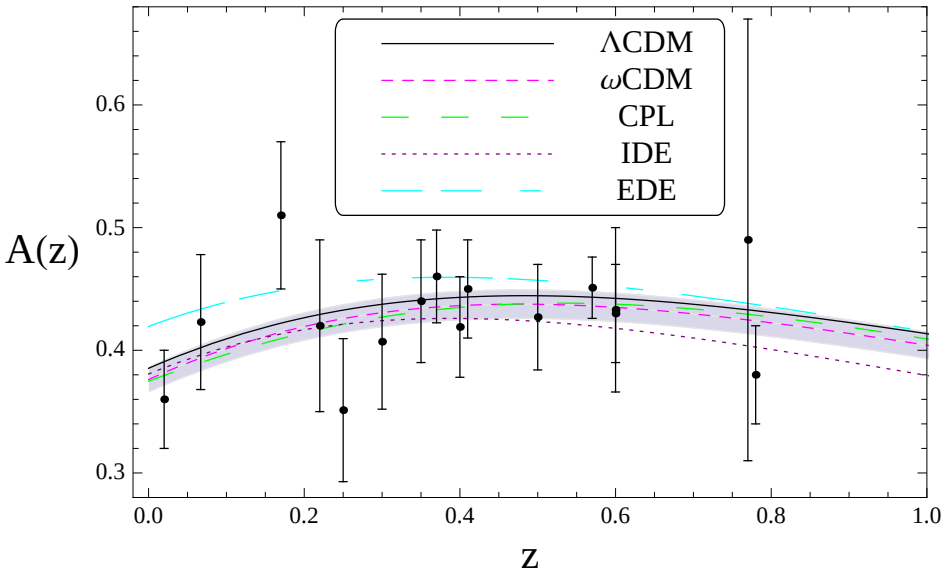

Figure 2. Growth parameter A(z) using the best fit parameters for different cosmological models. The region in gray shows the propagation of error 1σ of σ_8 for $\omega CDM model$.

The linear Growth Factor Structure $D(t)$ of the amplitude follows a simple differential equation (3.24). Through of the Growth Rate Data $f(a) \equiv a\dot{D}(a)/D(a)$ we get an observational stimate. We use the Growth Parameter $A(z) = f(z)\sigma_8(z)$ to constrain cosmological models through:

$$\chi^2_{GF} = \sum_{i=1}^{n} \frac{(A(z) - A_{obs}(z_i))^2}{\sigma_i^2} \tag{3.25}$$

where $A_{obs}(z_i)$ is the observed structure factor and $\sigma_8(z)$ is rms mass fluctuations in $8h^{-1}$ Mpc spheres. The growth structure data used in this paper are obtained from the following projects: PSCz, 2dF, VVDS, SDSS, 6dF, 2MASS, BOSS and WiggleZ galaxy surveys (Table 12, appendix B). As $\sigma_8(z) = \sigma_8^0 D(z)/D(0)$ then we can use σ_8^0 as a free parameter. The

observable Growth Parameter $A_{obs}(z)$ also accounts the Alcock-Paczynski effect in redshift-space distortions. Figure 2 shows the results of analysis, where the gray area is the error propagation to $1-\sigma$ for ωCDM model using the constrain on σ_8. In this paper an independent constraint on σ_8 was performed for each cosmological model and whose best fit was the one for the ΛCDM model, with a value of $\sigma_8 = 0.742 \pm 0.019$ (See Figure 3). As complementary tests we use Mass Gas Fracction (f_{gas}), GRBs, Strong Gravitational Lensing and SNIa (Union2.1) (See appendix A).

4 Method and data analysis

4.1 Maximum likelihood $\mathcal{L}_{max}$ and confidence level σ_i.

Maximum likelihood $\mathcal{L}_{max}$, is the procedure of finding the value of one or more parameters for a given statistic which makes the known likelihood distribution a maximum. The maximum likelihood estimate for the best fit parameters Θ_i^m is

$$\mathcal{L}_{max}(\Theta_i^m) = exp\left[-\frac{1}{2}\chi^2_{min}(\Theta_i^m)\right] \tag{4.1}$$

If $\mathcal{L}_{max}(\Theta_i^m)$ has a Gaussian errors distribution, then

$$\chi^2_{min}(\Theta_i^m) = -2\ln \mathcal{L}_{max}(\Theta_i^m), \tag{4.2}$$

which is our case [10]. So, for our analysis:

$$\chi^2_{min} = \chi^2_{CMB} + \chi^2_{BAO} + \chi^2_{GF} + \chi^2_{SNIa} + \chi^2_{GRBs} + \chi^2_{GC} + \chi^2_{SGL} \tag{4.3}$$

Table 7 presents the main results of cosmological parameters derived from the free parameters constrained in this study with all observational data.

Par	ΛCDM	ωCDM	CPL	IDE	EDE
H_0	69.58 ± 0.22	69.46 ± 0.21	69.53 ± 0.22	68.73 ± 0.28	68.51 ± 0.29
t_0	14.064 ± 0.044	14.087 ± 0.042	14.073 ± 0.045	14.236 ± 0.059	14.283 ± 0.0614
Ω_{r_0}	$8.613 \pm 0.054 \times 10^{-5}$	$8.651 \pm 0.053 \times 10^{-5}$	$8.634 \pm 0.056 \times 10^{-5}$	$8.835 \pm 0.073 \times 10^{-5}$	$8.893 \pm 0.076 \times 10^{-5}$
Ω_{γ_0}	$5.100 \pm 0.032 \times 10^{-5}$	$5.118 \pm 0.031 \times 10^{-5}$	$5.108 \pm 0.33 \times 10^{-5}$	$5.226 \pm 0.43 \times 10^{-5}$	$5.261 \pm 0.045 \times 10^{-5}$
Ω_{ν_0}	$3.521 \pm 0.022 \times 10^{-5}$	$3.533 \pm 0.021 \times 10^{-5}$	$3.526 \pm 0.022 \times 10^{-5}$	$3.608 \pm 0.029 \times 10^{-5}$	$3.632 \pm 0.031 \times 10^{-5}$
ω_{m_0}	0.14007 ± 0.00088	0.14047 ± 0.00085	0.14005 ± 0.00091	0.1547 ± 0.0013	0.1529 ± 0.0013
ω_{b_0}	0.02178 ± 0.00014	0.02171 ± 0.00013	0.02175 ± 0.00014	0.02129 ± 0.00017	0.02112 ± 0.00018
Ω_{X_0}	0.7095 ± 0.0054	0.7126 ± 0.0053	0.7182 ± 0.0063	0.6693 ± 0.0061	0.6701 ± 0.0068
ρ_{cri_0}	$9.101 \pm 0.057 \times 10^{-30}$	$9.070 \pm 0.055 \times 10^{-30}$	$9.088 \pm 0.058 \times 10^{-30}$	$8.881 \pm 0.073 \times 10^{-30}$	$8.823 \pm 0.075 \times 10^{-30}$
ρ_{X_0}	$6.457 \pm 0.041 \times 10^{-30}$	$6.463 \pm 0.039 \times 10^{-30}$	$6.527 \pm 0.042 \times 10^{-30}$	$5.944 \pm 0.049 \times 10^{-30}$	$5.912 \pm 0.051 \times 10^{-30}$
c_s	0.44965 ± 0.00056	0.44994 ± 0.00053	0.44977 ± 0.00057	0.45179 ± 0.00073	0.45233 ± 0.00075
z_{drag}	1019.15 ± 0.39	1019.02 ± 0.37	1019.08 ± 0.39	1019.11 ± 0.49	1018.66 ± 0.51
r_{drag}	152.09 ± 0.42	152.04 ± 0.38	152.13 ± 0.41	146.78 ± 0.88	148.14 ± 0.97
z_{cmb}	1092.52 ± 0.13	1092.66 ± 0.12	1092.56 ± 0.13	1094.61 ± 0.17	1094.68 ± 0.18

Table 7. Derived parameters for different cosmological dark energy models. We assume $\Omega_{b_0} = 0.045$ [55] and $N_{eff} = 3.04$ [1] for all cosmological models.

4.2 Fisher matrix, error propagation and uncertainties.

The Fisher matrix is widely used in the analysis of the constraint of cosmological parameters from different observational data sets [6, 89]. They encode the Gaussian uncertainties of the several parameters Θ_i^m. Given the best fit χ^2_{min}, the Fisher matrix can be calculeted as:

$$F_{ij} = \frac{1}{2}\frac{\partial^2 \chi^2_{min}}{\partial p_i \partial p_j}, \tag{4.4}$$

where p_i and p_j are the set of free parameters in each cosmological model. In the extended form we have:

$$[F] = \frac{1}{2}\begin{bmatrix} \frac{\partial^2}{\partial p_1^2} & \frac{\partial^2}{\partial p_1 \partial p_2} & \cdots & \frac{\partial^2}{\partial p_1 \partial p_n} \\ \frac{\partial^2}{\partial p_2 \partial p_1} & \frac{\partial^2}{\partial p_2^2} & \cdots & \frac{\partial^2}{\partial p_2 \partial p_n} \\ \cdot & \cdot & \cdot & \cdot \\ \cdot & \cdot & \cdot & \cdot \\ \cdot & \cdot & \cdot & \cdot \\ \frac{\partial^2}{\partial p_n \partial p_1} & \frac{\partial^2}{\partial p_n \partial p_2} & \cdots & \frac{\partial^2}{\partial p_n^2} \end{bmatrix} \chi^2_{min}(p_1, p_2, ..., p_n). \tag{4.5}$$

where $\chi^2_{min}(p_1, p_2, ..., p_n) = \chi^2_{min}(\Theta_1^m, \Theta_2^m, ..., \Theta_n^m)$, for the present analysis. The inverse of the Fisher matrix is the covariance matrix:

$$[C_{cov}] = [F]^{-1} = \begin{bmatrix} \sigma_1^2 & \sigma_{12} & \cdots & \sigma_{1n} \\ \sigma_{21} & \sigma_2^2 & \cdots & \sigma_{2n} \\ \cdot & \cdot & \cdot & \cdot \\ \cdot & \cdot & \cdot & \cdot \\ \cdot & \cdot & \cdot & \cdot \\ \sigma_{n1} & \sigma_{n2} & \cdots & \sigma_n^2 \end{bmatrix}, \tag{4.6}$$

where σ_i and σ_j are the uncertainties associated with each cosmological parameters p_i and p_j, to a level of statistical confidence of 1σ. The uncertainties are obtained as $\sigma_i = \sqrt{Diag\,[C_{cov}]_{ij}}$.

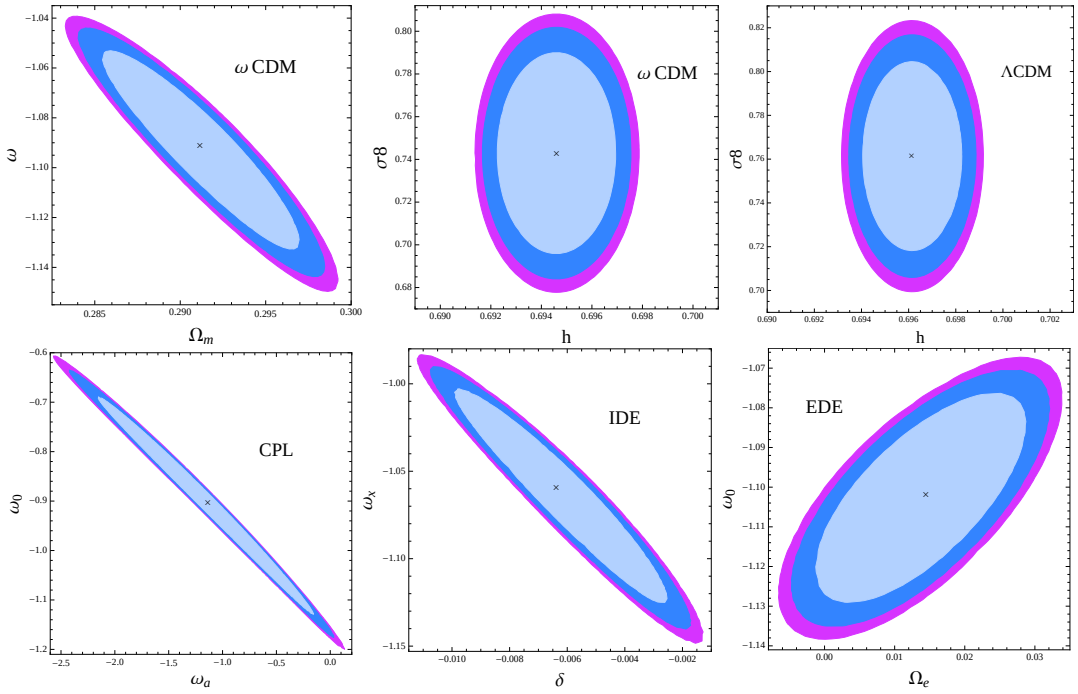

Figure 3. Diagrams of statistical confidence, marginalizing different cosmological parameters at 1σ, 2σ and 3σ, with all observational tests (CMB+BAO+SNIa+GRBs+GF+GC+SGL)

Table 3 presents statistical confidence diagrams obtained during this study, for each of the cosmological models of dark energy dynamics. In this paper we adopt the Figure of Merit Science Working Group (FoMSWG), proposed by the Joint Dark Energy Mission (JDEM), which it is a mission planned by NASA and Departamente of Energy (DOE) in USA for launch this year (2016)[1] (It is still in the study phase). The main goal of this mission is to test the properties of dark energy following the guidelines of the Dark Energy Task Force (DEFT) [5], which was established by the Astronomy and Astrophysics Advisory Committee (AAAC) and the High Energy Physics Advisory Panel (HEPAP) as a joint sub-committee to advise the NASA, DOE and National Science Foundation (NSF) on future dark energy research [5]. Within the main tasks proposed for this observational mission include: 1) Determine whether the accelerating expansion of the universe is consistent with a cosmological constant. 2) Measure as well as possible any sign of evolution with time of the density of dark energy. 3) Search for possible failure of general relativity comparing the effects of dark energy on the expansion with the effect of the same on the growth of structures at different scales. This work maintains the same spirit of the DEFT, especially in points a) and b), as shown by the results of the following sections.

4.3 Statistical discrimination models.

As mentioned before, we must give tight constraints on the parameters of the several models to discern among them which one is the most favored by the observations. To do that is not enough to calculate the best fit, we need to compare the models with each other using an appropriate statistical criterion. In this paper we use the Akaike information criterion (AIC; [3]) and the Bayesian information criterion (BIC; [73]), which allow to compare cosmological models with different degrees of freedom, with respect to the observational evidence and the set of parameters [57]. The AIC and BIC can be calculated as

$$AIC = -2\ln\mathcal{L}_{max} + 2k, \tag{4.7}$$

$$BIC = -2\ln\mathcal{L}_{max} + k\ln N, \tag{4.8}$$

where $\mathcal{L}_{max}$ is the maximum likelihood of the model under consideration, k is the number of parameters. It is worthy to note that BIC considers the number N of data points used in the fit. Thus, it imposes a strict penalty against extra parameters for any set of data $\ln N > 2$. The prefered model is that which minimizes AIC and BIC. However, the absolute values of them are not of interest, only the relative values between the different models. Therefore the "strength of evidence" can be characterized in the form $\Delta AIC = AIC_i - AIC_{min}$ $\Delta BIC = BIC_i - BIC_{min}$, where the subindex i refers to value of AIC (BIC) for model i and AIC_{min} (BIC_{min}) is the minimum value of AIC (BIC) among all the models [24, 70]. We give the judgements for both criterion in Tables 8 and 9

Thus, if we have a set of models of dark energy first we should estimate the best fit χ^2. Then we can apply the AIC and BIC to identify which model is the prefered one by the observations hence to the nature of dark energy. We also use the $\chi^2_{red} = \chi^2_{min}/\nu$ as criterion of good-fitting, for which the degrees of freedom are given by $\nu = N - k$, where the best model is that one whose value of χ^2_{red} is closet to one.

[1] http://science.nasa.gov/missions/jdem/

ΔAIC	Level of Empirical Support For Model i
$0-2$	Substantial
$4-7$	Considerably Less
>10	Essentially None

Table 8. ΔAIC criterion.

ΔBIC	Evidence Against Model i
$0-2$	Not Worth More Than A Bare Mention
$2-6$	Positive
$6-10$	Strong
>10	Very Strong

Table 9. ΔBIC criterion.

Model	k	χ^2_{min}	χ^2_{red}	AIC	ΔAIC	BIC	ΔBIC
ω CDM	5	809.860	1.106	819.860	0.00	842.872	0.00
Λ CDM	4	821.812	1.121	829.812	9.95	848.222	5.35
CPL	6	810.738	1.109	822.738	2.88	850.353	7.48
IDE	6	888.975	1.216	900.975	81.12	928.591	85.72
EDE	6	893.022	1.221	905.022	85.16	932.637	89.801

Table 10. Comparison of the different cosmological models with the ΔAIC y ΔBIC criterions using all complementary tests ($d_{A,c} + f_{gas} + BAO + CMB + SNIa + SL$). The ωCDM model is the most favored model by these criterios.

Table 10 shows the values of χ^2_{min}, AIC and BIC for the DE models from all cosmological tests. Notice that the ωCDM model gives the lowest value of AIC and BIC, therefore, we concluded that is the cosmological model most favored by observational data, as it can also be analyzed in Table 7. The ΔAIC and ΔBIC values for the other models are measured with respect to ωCDM. Following [75], we can classify the DE models in four groups: group 1, the model that shows a substantial level of empirical support and not worth more than a bare mention of evidence against to ωCDM; group 2, considerably less level of empirical support and some positive evidence against to ΛCDM; group 3, substantial level of empirical support and some strong evidence against to CPL model; group 4, essentially none substantial level of empirical support and very strong evidence against to IDE and EDE models.

5 Deceleration parameter

In this section we introduce of the most popular cosmological tests, which can help us to uncover some signs of the nature of dynamic dark energy.

It is natural to describe the kinematics of the cosmic expansion through the Hubble parameter $H(t)$ an and its dependence on time, i.e. the deceleration parameter $q(t)$. Following to [21] the scale factor $a(t)$ expands into a Taylor series around the current time (t_0) as:

$$\frac{a(t)}{a(t_0)} = 1 + \frac{H_0}{1!}[t-t_0] - \frac{q_0}{2!}H_0^2[t-t_0]^2 + \frac{j_0}{3!}H_0^3[t-t_0]^3 + \frac{s_0}{4!}H_0^4[t-t_0]^4 + ..., \quad (5.1)$$

where in general we can have a kinematic description of the cosmic expasion through the set of parameters:

$$H(t) \equiv \frac{1}{a}\frac{da}{dt}; \quad q(t) \equiv -\frac{1}{a}\frac{d^2a}{dt^2}H(t)^{-2}; \quad j(t) \equiv \frac{1}{a}\frac{d^3a}{dt^3}H(t)^{-3}; \quad s(t) \equiv \frac{1}{a}\frac{d^4a}{dt^4}H(t)^{-4}. \quad (5.2)$$

To characterize whether the universe is currently accelerated or decelerated, the history of expansion is fit through deceleration parameter $q(z) \equiv -\ddot{a}(z)/a(z)H(z)^2$. If $q(z) > 0$, $\ddot{a}(z) < 0$; then the expansion decelerate, as expected due to gravity (i.e. dark matter, baryonic matter, radiation). The discovery that the universe is currently accelerating, already has about one decade and a half old [65] [69]. The simplest explanation for the accelerating universe is the cosmological constant Λ, however, there is still no compelling theoretical explanation based on physical foreground and not only phenomenological. To take account information about the dynamics of the expansion we to use (2.2) and (5.2), then we obtain

$$q(z) = \frac{1+z}{E(z)}\frac{dE(z)}{dz}, \quad (5.3)$$

which directly depends on the cosmological model and its matter-energy content. In general, if $\Omega_X \neq 0$ is sufficiently large (i.e. $\Omega_X > \Omega_m$), then $q(z) < 0$ and $\ddot{a}(z) > 0$, which corresponds to an expansion accelerated the universe as shown by observational data at present, which also indicates a cosmological constant different from zero (see Table 7). If the acceleration of the universe is driven by a new fluid, then it is important to identify signs to determine if the energy density of the fluid is constant or dynamic.

Model	χ^2_{min}	Parameters
Λ CDM	2.69	h=0.5822, Ω_m=0.2232, Ω_k=-0.0107
ω CDM	2.63	h=0.9197, Ω_m=0.3203, Ω_k=-0.3347, ω=-0.9048
CPL	2.68	h=0.6742, Ω_m=0.2839, Ω_k=-0.0425, ω_a=-1.0254, ω_0=-0.8935
IDE	2.59	h=0.5931, Ω_m=0.4626, Ω_k=-1.1601, ω_x=-0.7085, δ=0.1069
EDE	2.61	h=0.8321, Ω_m=0.3807, Ω_k=-0.2711, ω_0=-0.9875, Ω_e= -0.1383

Table 11. The best fit values for the free parameters using the only BAO data set.

Figure 4 shows the plot of the deceleration parameter $q(z)$ using only data from BAO (See Table 11). As expected, the models studied give $q(z) < 0$ at late times and $q(z) > 0$ at earlier epoch, which means that the history of the expansion is slowed down in the past and speeded up at present. All cosmological models presents a redshift of transition (z_t) between the two periods (see Figure 4), however, all models of dynamical dark energy present an interesting behavior of slowing down of acceleration at low redshift (late times) using only data from BAO, which can be characterized through the change of sign of the parameter $j(z)$ (CPL: $j(z_{low}) \to 0$, when $z_{low} \sim 0.11$; IDE: $j(z_{low}) \to 0$, when $z_{low} \sim 0.00$; EDE: $j(z_{low}) \to 0$, when $z_{low} \sim 0.05$). We can interpret j(z) as the slope at each point of q(z), which indicates a change in acceleration. This result is consistent with the one presented by J. Barrow, R.

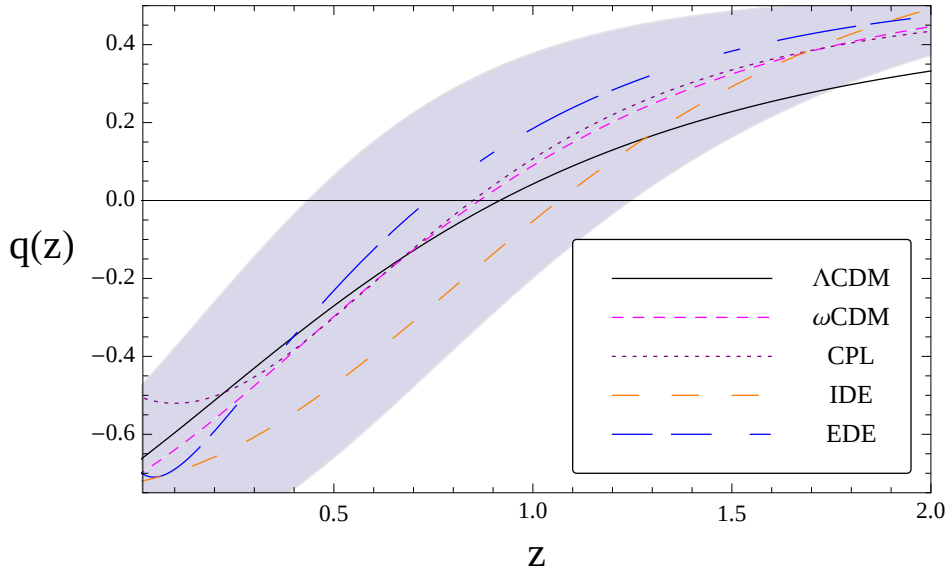

Figure 4. Desaceleration parameter vs redshift using only BAO data, where the gray region corresponds to the best fit to 1σ for ωCDM model, with error propagation only on $\Omega_m = 0.32 \pm 0.16$. It is shown the transition decelerated-accelerated ($q(z_t) = 0$) and the current value of (q_0) (ΛCDM ($z_t \sim 0.92$, $q_0 = -0.67$), ωCDM ($z_t \sim 0.86$, $q_0 = -0.70$), CPL ($z_t \sim 0.85$, $q_0 = -0.48$), IDE ($z_t \sim 1.06$, $q_0 = -0.72$), EDE ($z_t \sim 0.73$, $q_0 = -0.68$)). Note the strange behavior of the deceleration parameter to later times for models of dynamical dark energy (CPL, IDE, EDE).

Bean and J. Magueijo [13], who raises the possibility of a scenario consistent with the current accelerating universe and does not involve an eternal accelerated expansion. In [21] extensive analysis it is made of this possibility. This can be also a clear behavior of dynamical dark energy at low redshift in this models with variation of the density of dark energy over time.

6 Summary and discussion

In this paper we perform the study of the history of the of cosmic expansion through the H(z), q(z) and j(z) parameters with data from SDSS, WiggleZ, BOSS and CMASS, using BAO distance ratio scale $r_s/D_v(z)$. We find new evidence presented in previous work, showing peculiar behavior of the deceleration parameter q(z) in later times ($z_{low} < 0.5$), which indicates through the change of sign of the parameter $j(z)$ ($+\rightarrow$ -), that the universe could decelerate in the near future (Figure 4). This phenomenon raises the possibility that an accelerated expansion does not imply the eternal accelerated expansion, even in the presence of dark energy. This anomalous behavior is present only in models with dark energy density varying with the time. This behavior is possibly due to the dynamics of the dark energy density in this class of cosmological models, which in principle can be a sign of evolution with time of the density of dark energy and could distinguish from a constant density of dark energy. However, Figure 4 shows that Λ still can not be ruled out in this analysis, since all models are in the region of error propagation to 1σ of ωCDM and would have to make a deeper analysis , for example by including other observational evidence for better restriction, which will be presented in next paper.

In the study of the comparing different cosmological models of dark energy we use the most recent observational data. This data includes statistical combination of CMB (Plank 13 + WMAP 9), BAO (SDSS, WiggleZ, BOSS and CMASS), A(z) (PSCz, 2dF, VVDS, SDSS, 6dF, 2MASS, BOSS and WiggleZ), SNIa (Union 2.1), GRBs, SGL and f_{gas}. By using these data sets, we obtained the best-fit parameters for different cosmological models. We use the information criteria including the ΔAIC and the ΔBIC, to compare different models and to see which is the most favored by current observational data. Our analysis shows that ωCDM dark energy model is preferred by Bayesian and Akaike criterion. By first time we report that observational data are in favor of the cosmological model ωCDM and very close to being in favor of models of dynamical dark energy as Chevalier-Polarski-Linder model, which is better than ΛCDM for ΔAIC (See Table 10). In Table 2 and Figure 3 we can see that ΛCDM model ($\omega = -1$) is excluded to a level of statistical confidence of 3σ ($\omega = -1.091^{+0.051}_{-0.059}$) combining all observational data for the present analysis and also from all other cosmological models. We include the parameter information that are commonly used in the characterization of models of the universe, with error propagation 1 *sigma* from the constraint of free parameters for each cosmological models of dark energy presented in Table 7.

Assuming that general relativity is the correct theory of gravity, we used measures of the growth parameter $A(z)$ (See Table Appendix B) to put independent constraints on variance in mass flucuaciones $\sigma_8 = 0.742 \pm 0.019$. We are able to break the degeneracy between Ω_m and σ_8, through the use of the equation (3.24), to thereby achieve a good independent constraint. Constrain as best as possible this parameter is very important in cosmology because through its the normalization of the power spectrum of the matter is done.

Acknowledgments

A. Bonilla wish to express their gratitude to Universidad Distrital FJDC for the academic support and funding. A. Bonilla and J. Garcia wishes to thank to the guest lecturers for his comments and suggestions to this work within the framework of *I Workshop on Current Challenges in Cosmology: Inflation and the Origin of the CMB Anomalies* [2], *I Simposio Andino de Astrofísica Relativista* [3] and the professors Yehuda Hoffman and Stefan Gottloeber within the framework of academic event *Escuela Andina de Cosmología* [4]. A. Bonilla and J. Garcia also wish give special thanks to *Dr. Florian Beutler* for their appropriate comments about the most recent BAO data and *Dr. Santiago Vargas* (OAN, UNAL) for their cordial review of "systematic errors" in the preparation of this work.

A Section in Appendix

A.1 Gas mass fraction

Also we use 42 measurements of f_{gas} of galaxy cluster from [8]. Thus, the χ^2 formula to test the different cosmological models we have

[2] http://cosmology.univalle.edu.co
[3] https://eventos.redclara.net/indico/event/503/
[4] http://forero.github.io/AndeanCosmologySchool/

$$\chi^2_{f_{gas}}(z_i,\Theta) = \sum_{i=1}^{42} \frac{[f_{gas}^{\Lambda CDM}(z_i,\Theta) - f_{gas}(z_i,\Theta)]^2}{\sigma^2_{f_{gas}}} + \left(\frac{\Omega_b h^2 - 0.0214}{0.0020}\right)^2 + \left(\frac{h-0.72}{0.08}\right)^2 + \left(\frac{b-0.824}{0.089}\right)^2 \tag{A.1}$$

where f_{gas} is observational gas mass fraction data [8], $f_{gas}^{\Lambda CDM}(z)$ is the gas mass fraction of the cosmological models tested and $\sigma_{f_{gas}}$ is the error of data [7]. In the former expression we have considered constant values for $b = 0.824$ [45] and $\Omega_b = 0.045$ [55] .

A.2 SNIa

Here, we use the Union 2.1 sample which contains 580 data. The SNIa data give the luminosity distance $d_L(z) = (1+z)r(z)$. We fit the SNIa with the cosmological model by minimizing the χ^2 value defined by

$$\chi^2_{SNIa} = \sum_{i=1}^{580} \frac{[\mu(z_i) - \mu_{obs}(z_i)]^2}{\sigma^2_{\mu_i}}, \tag{A.2}$$

where $\mu(z) \equiv 5\log_{10}[d_L(z)/\mathtt{Mpc}] + 25$ is the theoretical value of the distance modulus, and μ_{obs} is the corresponding observed one.

A.3 Gammay-ray Burst Data

We add gammay-ray burst (GRB) data to our analysis, since these are complementary in redshift range to the SNIa data. We use GRB data in the form of the model-independent GRB distance measurements from [85], which were derived from the data of 69 GRBs with $0.17 \leq z \leq 6.6$ from [72] and recently used in [23] to constrain holographic dark energy models. The GRB data are included in our analysis by adding the following term to the given model:

$$\chi^2_{GRB} = [\Delta\bar{r}_p(z_i)] \,.(C^{-1}_{GRB})_{ij}.\, [\Delta\bar{r}_p(z_i)]\,, \tag{A.3}$$

where $\Delta\bar{r}_p(z_i) = \bar{r}_p^{data}(z_i) - \bar{r}_p(z_i)$ and $\bar{r}_p(z_i)$ is given by

$$\bar{r}_p(z_i) = \frac{r_p(z)}{r_p(0.17)}, r_p(z) = \frac{(1+z)^{1/2}}{z}\frac{H_0}{ch}r(z) \tag{A.4}$$

where $r(z)$ is the comoving distance at z.

A.4 Gravitational Lensing

The fit of the theoretical models to strong lensing observations can be found by the minimization of

$$\chi^2_{SL} = \sum_{i=1}^{80} \frac{\left(\mathcal{D}_i^{obs} - \mathcal{D}_i^{th}\right)^2}{\sigma^2_{\mathcal{D},i}} \tag{A.5}$$

where the sum is over the sample and $\sigma^2_{\mathcal{D},i}$ denotes the variance of $\mathcal{D}_i^{obs}$. Here, we use a sample of 80 strong lensing systems by [18, 19] which contains 70 data points from SLACS and LSD and 10 data points from galaxy clusters.

B Section in Appendix

Index	z	$A_{obs}(z_i)$	Refs.
1	0.02	0.360 ± 0.040	[53]
2	0.067	0.423 ± 0.055	[16]
3	0.17	0.510 ± 0.060	[63, 76]
4	0.35	0.440 ± 0.050	[76, 82]
5	0.77	0.490 ± 0.180	[50, 76]
6	0.25	0.351 ± 0.058	[71]
7	0.37	0.460 ± 0.038	[71]
8	0.22	0.420 ± 0.070	[20]
9	0.41	0.450 ± 0.040	[20]
10	0.60	0.430 ± 0.040	[20]
11	0.78	0.380 ± 0.040	[20]
12	0.57	0.427 ± 0.066	[68]
13	0.30	0.407 ± 0.055	[83]
14	0.40	0.419 ± 0.041	[83]
15	0.50	0.427 ± 0.043	[83]
16	0.60	0.433 ± 0.067	[83]

Table 12. Summary of the observed growth rate and references.

References

[1] Ade, P.A.R. *et al.*, *Planck 2013 results. XVI. Cosmological parameters*, 2013, [arXiv:1303.5076].

[2] Planck Collaboration, Ade, P. A. R., Aghanim, N., et al. 2015, arXiv:1502.01589

[3] Akaike H., *A New Look at the Statistical Model Identification*, 1974, *IEEE Transactions on Automatic Control*, 19, 716.

[4] Albrecht, A., Bernstein, G., Cahn, R., et al. 2006, arXiv:astro-ph/0609591

[5] Albrecht, A., Bernstein, G., Cahn, R., et al. 2006, arXiv:astro-ph/0609591

[6] Albrecht A., Amendola L., Bernstein G., Clowe D., Eisenstein D., Guzzo L., Hirata C. and Huterer D. *et al.*, *Findings of the Joint Dark Energy Mission Figure of Merit Science Working Group*,2009, [arXiv:0901.0721].

[7] S. W. Allen, R. W. Schmidt, H. Ebeling, A. C. Fabian and L. van Speybroeck, *Constraints on dark energy from Chandra observations of the largest relaxed galaxy clusters*, 2004, MNRAS **353**, 457, [astro-ph/0405340].

[8] S. W. Allen, D. A. Rapetti, R. W. Schmidt, H. Ebeling, G. Morris and A. C. Fabian, *Improved constraints on dark energy from Chandra X-ray observations of the largest relaxed galaxy clusters*, 2007, MNRAS **383**, 879 (2008), [arXiv:0706.0033 [astro-ph]].

[9] L. Amendola,*Coupled quintessence*, 2000, Phys. Rev. D **62**, 043511 (2000), [astro-ph/9908023].

[10] R. Andrae, T. Schulze-Hartung and P. Melchior,"Dos and don'ts of Orangeuced chi-squaOrange," arXiv:1012.3754 [astro-ph.IM].

[11] Armendariz-Picon, C.; Mukhanov, V.; Steinhardt, P. J., *A Dynamical Solution to the Problem of a Small Cosmological Constant and Late-time Cosmic Acceleration*, 2000, PRL, 85, 4438, [astro-ph/0004134].

[12] Armendariz-Picon, C.; Mukhanov, V.; Steinhardt, P. J., *Essentials of k-essence*, 2000, PRD, 63, 103510, [astro-ph/0006373].

[13] Barrow, J. D., Bean, R., & Magueijo, J. 2000, MNRAS, 316, L41

[14] Bassett, B., & Hlozek, R. 2010, Dark Energy: Observational and Theoretical Approaches, 246

[15] Beutler F. et al., 2011, MNRAS, 416, 3017

[16] F. Beutler, et al., Mon. Not. Roy. Astron. Soc., **423**, 3430 (2012)

[17] Beutler, F., Blake, C., Koda, J., et al. 2016, MNRAS, 455, 3230

[18] Biesiada, M., *Strong lensing systems as a probe of dark energy in the universe*, 2006, PRD, 73, 023006.

[19] Biesiada, M.; Piórkowska, A.; Malec, B., *Cosmic equation of state from strong gravitational lensing systems*, 2010, MNRAS, 406, 1055, [arXiv:1105.0946].

[20] C. Blake et al., Mon. Not. Roy. Astron. Soc., **415**, 2876 (2011)

[21] Bolotin, Y. L., Erokhin, D. A., & Lemets, O. A. 2012, Physics Uspekhi, 55, A02

[22] Bond J. R., Efstathiou G., Tegmark M., 1997, MNRAS 291, L33

[23] Bonilla Rivera, A., & Castillo Hernandez, J. E. 2016 *Constraints On Holographic Cosmological Models From Gamma Ray Bursts*, arXiv:1601.00183

[24] Burnham K. P. & Anderson D. R. 2003, *Model Selection and Multimodel Inference*, *Technometrics*, 45, 181.

[25] R. -G. Cai and A. Wang, *Cosmology with interaction between phantom dark energy and dark matter and the coincidence problem*, 2005, JCAP **0503**, 002, [hep-th/0411025].

[26] G. Caldera-Cabral, R. Maartens and L. A. Urena-Lopez,*Dynamics of interacting dark energy*, 2009, Phys. Rev. D **79**, 063518 [arXiv:0812.1827 [gr-qc]].

[27] Caldwell, R. R., Dave, R. & Steinhardt P. J., *Cosmological Imprint of an Energy Component with General Equation of State*, 1998, Phys. Rev. Lett. **80**, 1582, [astro-ph/9708069].

[28] Caldwell, R. R., *A Phantom Menace? Cosmological consequences of a dark energy component with super-negative equation of state*, 2002, Phys. Rev. Lett. B, 545, 23, [astroph/9908168].

[29] Cárdenas, V.; Bernal, C.; Bonilla, A., *Cosmic slowing down of acceleration using* f_{gas}, 2013, submitted to MNRAS, [arXiv:1306.0779].

[30] Cárdenas, V. H., & Rivera, M. 2012, American Institute of Physics Conference Series, 1471, 88

[31] Cárdenas, V. H., & Rivera, M. 2012, Physics Letters B, 710, 251

[32] Carmeli, M., & Kuzmenko, T. 2001, 20th Texas Symposium on relativistic astrophysics, 586, 316

[33] Chevallier M and Polarski D, *Accelerating Universes with Scaling Dark Matter*, 2001,*Int. J. Mod. Phys. D* 10, 213, [gr-qc/0009008].

[34] Chiba, T., Okabe, T. and Yamaguchi, M., *Kinetically driven quintessence*, 2000, Phys. Rev. Lett. D, **62**, 023511, [astro-ph/9912463].

[35] Cohen, A. G., Kaplan, D.B. & Nelson, A.E., *Effective Field Theory, Black Holes, and the Cosmological Constant*, 1999, Phys. Rev. Lett., 82, 4971, [arXiv:hep-th/9803132v2].

[36] Cole, S., Percival, W. J., Peacock, J. A., et al. 2005, MNRAS, 362, 505

[37] Conley et al. *Supernova Constraints and Systematic Uncertainties from the First Three Years of the Supernova Legacy Survey* 2011, Ap. J. Suppl.192, 1, [arXiv:1104.1443].

[38] Copeland, E. J., Sami, M., & Tsujikawa, S., *Dynamics of dark energy*, 2006, IJMP D **15**, 1753, [arXiv:hep-th/0603057].

[39] N. Dalal, K. Abazajian, E. E. Jenkins and A. V. Manohar, *Testing the cosmic coincidence problem and the nature of dark energy*, 2001, Phys. Rev. Lett.**87**, 141302, [astro-ph/0105317].

[40] Doran & Robbers, *Early Dark Energy Cosmologies*, 2006, JCAP, 6, 26, [astro-ph/0601544].

[41] Durrer, R. The Cosmic Microwave Background, Cambridge University Press, 2008.

[42] G. R. Dvali, G. Gabadadze and M. Porrati,*4-D gravity on a brane in 5-D Minkowski space*, 2000, Phys. Lett. B **485**, 208, [hep-th/0005016].

[43] Eisenstein D. J., Hu W., 1998, ApJ, 496, 605

[44] Eisenstein, D. J., Zehavi, I., Hogg, D. W., et al. 2005, Ap. J., 633, 560

[45] V. R. Eke, J. F. Navarro and C. S. Frenk, *The Evolution of x-ray clusters in low density universes*, 1998, Astrophys. J. **503**, 569, [astro-ph/9708070].

[46] Frieman, J. A., Turner, M. S., & Huterer, D. 2008, ARA&A, 46, 385

[47] García-Aspeitia, M. A., Magaña, J. and Matos T., *Braneworld model of dark matter: structure formation*, 2012, GReGr, **44**, 581, [arXiv:1102.0825v3].

[48] Z. K. Guo, Y. S. Piao, X. M. Zhang & Y. Z. Zhang, *Cosmological Evolution of a Quintom Model of Dark Energy*, 2005, Phys. Lett. B608, 177, [astro-ph/0410654]. Planck 2013 results. XXIX. The Planck catalogue of Sunyaev-Zeldovich sources

[49] Z. -K. Guo, N. Ohta and S. Tsujikawa, *Probing the Coupling between Dark Components of the Universe*, 2007, Phys. Rev. D **76**, 023508, [astro-ph/0702015].

[50] L. Guzzo *et al.*, Nature **451**, 541 (2008)

[51] G. Hinshaw, D. Larson, E. Komatsu, D. N. Spergel, C. L. Bennett, J. Dunkley, M. R. Nolta and M. Halpern *et al.* [WMAP Collaboration],*Nine-Year Wilkinson Microwave Anisotropy Probe (WMAP) Observations: Cosmological Parameter Results*, 2012, accepted to Astrophys. J. Suppl. [arXiv:1212.5226].

[52] Hogg DW., *Distance measures in cosmology*, 1999, [astro-ph/9905116].

[53] M. J. Hudson and S. J. Turnbull, Astrophys. J. Let. **715**, 30 (2012)

[54] Hu W., Sugiyama N., 1996, ApJ 471, 542

[55] D. Kirkman, D. Tytler, N. Suzuki, J. M. O'Meara and D. Lubin, *The Cosmological baryon density from the deuterium to hydrogen ratio towards QSO absorption systems: D/H towards Q1243+3047*, 2003, Astrophys. J. Suppl. **149**, 1, [astro-ph/0302006].

[56] E. W. Kolb, M. S. Turner. The Early Universe, Addison-Wesley, 1989.

[57] Liddle A. R., *How many cosmological parameters?*, 2004, MNRAS 351, L49-L53, [astro-ph/0401198v3].

[58] Linder E. V., *Mapping the Dark Energy Equation of State*, 2003, *Phys. Rev. Lett.*, 90, 091301, [astro-ph/0311403].

[59] Magaña, J., Cárdenas, V. H., & Motta, V. 2014, JCAP, 10, 017

[60] S. Nesseris and L. Perivolaropoulos, *Crossing the Phantom Divide: Theoretical Implications and Observational Status*, 2007, JCAP **0701**, 018, [astro-ph/0610092].

[61] Nesseris, S., Blake, C., Davis, T., & Parkinson, D. 2011, JCAP, 7, 037

[62] Parker, L. and Raval, A., *Non-perturbative effects of vacuum energy on the recent expansion of the universe*, 1999, Phys. Rev. D, **60**, 063512, [arXiv:gr-qc/9905031].

[63] W. J. Percival, et al., Mon. Not. Roy. Astron. Soc., **353**, 1201 (2004)

[64] Percival W. J. et al., 2010, MNRAS, 401, 2148

[65] Perlmutter, S., Aldering, G., Goldhaber, G., et al. 1999, Ap. J., 517, 565

[66] Pettorino, V., Amendola, L., & Wetterich, C. 2013, Phys. Rev. **D**, 87, 083009

[67] Ratra, B. & Peebles, P. J. E., *Cosmological consequences of a rolling homogeneous scalar field*, 1988, Phys. Rev. D **37**, 3406.

[68] B. A. Reid et al., Mon. Not. Roy. Astron. Soc., **426**, 2719 (2012)

[69] Riess, A. G., Filippenko, A. V., Challis, P., et al. 1998, AJ, 116, 1009

[70] Robert E. K. Adrian E. R., *Bayes Factors*, 1995, *Journal of the American Statistical Association*, 90, 773.

[71] L. Samushia, W. J. Percival and A. Raccanelli, [arXiv:1102.1014] (2012)

[72] Schaefer, B. E. 2007, Ap. J., 660, 16.

[73] Schwarz, G., *Estimating the Dimension of a Model*, 1978, *The Annals of Statistics*, 6, 471.

[74] A. Shafieloo, V. Sahni and A. A. Starobinsky,*Is cosmic acceleration slowing down?*, 2009, Phys. Rev. **D**80, 101301, [arXiv:0903.5141].

[75] Shi K., Huang Y. & Lu T., *A comprehensive comparison of cosmological models from latest observational data*, 2012, MNRAS, **426**, 2452, [arXiv:1207.5875].

[76] Y-S. Song and W.J. Percival, J. Cosmol. Astropart. Phys., **10** (2009) 004

[77] Stabenau, H. F., & Jain, B. 2006, Phys. Rev. **D**, 74, 084007

[78] Steinhardt P. J., Wang L., Zlatev I., *Cosmological tracking solutions*, 1999, Phys. Rev. **D**, 59, 123504, [astro-ph/9812313].

[79] Susskind, L., *The world as a hologram*, 1995, JMPh 36, 6377, [arXiv:hep-th/9409089].

[80] 't Hooft, G., *"Dimensional Reduction in Quantum Gravity"*, 1993, [arXiv:gr-qc/9310026].

[81] 't Hooft, G., *"The Holographic Principle"*, 2001, [arXiv:hep-th/0003004].

[82] M. Tegmark *et al.*, Phys. Rev. D **74**, 123507 (2006)

[83] R. Tojeiro, et al., Mon. Not. Roy. Astron. Soc., **424**, 2339 (2012)

[84] Uzan, J.-P. 2006, arXiv:astro-ph/0605313

[85] Wang, Y. 2008, Phys. Rev. **D**, 78, 123532

[86] Weinberg, S., *The cosmological constant problem*, 1989, RMP 61, 1.

[87] Wetterich, C., *Cosmology and the fate of dilatation symmetry*, 1988, Nucl. Phys. B 302, 668.

[88] White, M. 2005, Astroparticle Physics, 24, 334

[89] Wolz, L., Kilbinger, M., Weller, J., & Giannantonio, T. 2012, JCAP, 9, 009

[90] Zhang, H., Li, X. Z. & Noh, H., *Semi-Holographic Universe*, 2010, Physics Letters B, **694**, 177.